Na^+- and Cl^--coupled active transport of nitric oxide synthase inhibitors via amino acid transport system $B^{0,+}$

Takahiro Hatanaka,[1] Takeo Nakanishi,[1] Wei Huang,[1] Frederick H. Leibach,[1] Puttur D. Prasad,[1,2] Vadivel Ganapathy,[1,2] and Malliga E. Ganapathy[3]

[1]Department of Biochemistry and Molecular Biology,
[2]Department of Obstetrics and Gynecology, and
[3]Department of Medicine, Medical College of Georgia, Augusta, Georgia, USA

Address correspondence to: Malliga E. Ganapathy, Department of Medicine, Division of Infectious Diseases, Medical College of Georgia, Augusta, Georgia 30912, USA.
Phone: (706) 721-7652; Fax: (706) 721-6608; E-mail: mganapat@mail.mcg.edu.

Received for publication December 20, 2000, and accepted in revised form February 26, 2001.

Nitric oxide synthase (NOS) inhibitors have therapeutic potential in the management of numerous conditions in which NO overproduction plays a critical role. Identification of transport systems in the intestine that can mediate the uptake of NOS inhibitors is important to assess the oral bioavailability and therapeutic efficacy of these potential drugs. Here, we have cloned the Na^+- and Cl^--coupled amino acid transport system $B^{0,+}$ ($ATB^{0,+}$) from the mouse colon and investigated its ability to transport NOS inhibitors. When expressed in mammalian cells, $ATB^{0,+}$ can transport a variety of zwitterionic and cationic amino acids in a Na^+- and Cl^--coupled manner. Each of the NOS inhibitors tested compete with glycine for uptake through this transport system. Furthermore, using a tritiated analog of the NOS inhibitor N^G-nitro-L-arginine, we showed that Na^+- and Cl^--coupled transport occurs via $ATB^{0,+}$. We then studied transport of a wide variety of NOS inhibitors in *Xenopus laevis* oocytes expressing the cloned $ATB^{0,+}$ and found that $ATB^{0,+}$ can transport a broad range of zwitterionic or cationic NOS inhibitors. These data represent the first identification of an ion gradient–driven transport system for NOS inhibitors in the intestinal tract.

J. Clin. Invest. **107**:1035–1043 (2001).

Introduction

Nitric oxide (NO) is an important regulatory molecule involved in a variety of physiological processes (1–3). This molecule is generated from L-arginine by nitric oxide synthases (NOS). Three distinct isoforms of NOS have been identified: neuronal NOS (nNOS or NOS I), inducible NOS (iNOS or NOS II), and endothelial NOS (eNOS or NOS III) (4, 5). Even though NO plays an essential role in many physiological processes, overproduction of NO is associated with a multitude of pathological conditions, including inflammation, septic shock, diabetes, and neurodegeneration (6–9). Blockade of NO production by inhibition of NOS may therefore have potential in the treatment of these pathological conditions. Since different isoforms of NOS are involved in different pathological conditions, selective inhibition of specific isoforms of NOS will become necessary to enhance the therapeutic use of this approach for differential treatment of these disorders. Several inhibitors have been identified that are selective for different NOS isoforms (10, 11). Use of these inhibitors has been shown to be beneficial in the treatment of diverse conditions associated with overproduction of NO in humans and in experimental animals (12, 13).

The therapeutic efficacy of NOS inhibitors is expected to be influenced markedly by the efficiency with which these inhibitors are taken up into the target cells for interaction with NOS. Furthermore, transport of these inhibitors in the intestine will influence their oral bioavailability. Therefore, information on the mechanisms of cellular uptake of NOS inhibitors is critical to assess their therapeutic potential. Most NOS inhibitors are structurally related to arginine, lysine, citrulline, and ornithine (10, 11). Consequently, amino acid transport systems play a critical role in the cellular uptake of NOS inhibitors. Multiple systems operate in mammalian cells to mediate the transport of amino acids and these transport systems differ markedly in substrate specificity, substrate affinity, driving forces, and tissue-expression pattern (14). Many of these transport systems have been recently cloned and functionally characterized (15, 16). There have been several studies in the past aimed at identifying the amino acid transport systems that mediate the uptake of NOS inhibitors (17–21). Two amino acid transport systems have been identified so far that are involved in the cellular uptake of NOS inhibitors. These are system y^+ and system L. Both are Na^+-independent transport systems and therefore exhibit only a weak capacity to concentrate their substrates, including the NOS inhibitors inside the cells. To our knowledge, no other amino acid transport system has been shown to be involved in the transport of NOS inhibitors. Recently, we initiated studies to determine the role of the amino acid trans-

port system $B^{0,+}$ ($ATB^{0,+}$) in the cellular uptake of NOS inhibitors (22). These studies have suggested that system $B^{0,+}$ may potentially participate in the transport of the NOS inhibitor N^G-nitro-L-arginine (L-NNA). System $B^{0,+}$ differs from system y^+ and system L in two important aspects. First, unlike systems y^+ and L that are specific for either cationic or zwitterionic amino acids, respectively, system $B^{0,+}$ can accept cationic as well as zwitterionic amino acids as substrates. This characteristic is important because there are cationic NOS inhibitors as well as zwitterionic NOS inhibitors that have been identified as specific inhibitors of different NOS isoforms. Second, system $B^{0,+}$ is a highly concentrative transport system, being energized by multiple driving forces (Na^+ gradient, Cl^- gradient, and membrane potential). Therefore, the ability of system $B^{0,+}$ to concentrate its substrates inside the cells is severalfold greater than that of systems y^+ and L. Since $B^{0,+}$ is expressed in the intestinal tract (16), this system has the potential to serve as a drug delivery system for NOS inhibitors. The present study was undertaken to investigate the transport of a wide variety of structurally diverse and isoform-specific NOS inhibitors via $ATB^{0,+}$ cloned from the mouse intestine.

Methods

Materials. [^{3}H]-Glycine was purchased from Moravek Biochemicals Inc. (Brea, California, USA) and [^{3}H]-L-NNA was purchased from Amersham Pharmacia Biotech (Piscataway, New Jersey, USA). All other radiolabeled amino acids were obtained from either NEN Life Science Products (Boston, Massachusetts, USA) or American Radiolabeled Chemicals Inc. (St. Louis, Missouri, USA). NOS inhibitors were obtained from either Sigma Chemical Co. (St. Louis, Missouri, USA) or Calbiochem-Novabiochem Corp. (San Diego, California, USA).

Cloning of mouse $ATB^{0,+}$. The SuperScript plasmid system (Life Technologies Inc., Rockville, Maryland, USA) was used to establish a unidirectional cDNA library with poly(A)$^+$ RNA isolated from mouse colon as described previously (23–25). The probe for library screening was prepared by RT-PCR using primers specific for mouse $ATB^{0,+}$ cDNA reported in the GenBank (accession no. AF161714). The primers were 5′-GTT GGC TAT GCA GTG GGA TT-3′ (sense) and 5′-GAG GCC AAG GAG AAA CAA AA-3′ (antisense), which corresponded to the nucleotide positions 396–415 and 1606–1625 in the cDNA sequence. RT-PCR was performed using the poly(A)$^+$ RNA prepared from mouse colon and the resulting product, approximately 1.2 kbp in size, was subcloned and sequenced to confirm its identity. This cDNA was labeled with [α-^{32}P]dCTP by random priming and used as a probe for screening the mouse colon cDNA library. Sequencing was done using an automated 377 Prism DNA sequencer (Perkin-Elmer Applied Biosystems, Foster City, California, USA). The longest positive clone (~3 kbp) was used for functional studies.

Northern blot analysis. The expression pattern of $ATB^{0,+}$ mRNA along the longitudinal axis of the mouse intestinal tract was investigated by Northern blot analysis. The entire small intestine was divided into four equal segments, the first segment representing the most proximal small intestine and the fourth segment representing the most distal small intestine. Poly(A)$^+$ mRNA was isolated from these four segments as well as from the cecum and colon and used for Northern blot analysis. The blot was hybridized sequentially under high-stringency conditions with [^{32}P]-labeled cDNA probes specific for mouse $ATB^{0,+}$, mouse peptide transporter 1 (PEPT1), and mouse β-actin.

Functional expression $ATB^{0,+}$ in HRPE cells. The functional expression was carried out using the vaccinia virus expression system (23–25). Transport measurements were made at 37°C for 15 minutes with radiolabeled amino acids or NOS inhibitors as substrates. The transport buffer was 25 mM HEPES/Tris (pH 7.5) containing 140 mM NaCl, 5.4 mM KCl, 1.8 mM $CaCl_2$, 0.8 mM $MgSO_4$, and 5 mM glucose. Endogenous transport activity was always determined in parallel using cells transfected with vector alone. With glycine as the substrate that was used in most of the experiments, the endogenous transport accounted for less than 5% of the transport measured in cells that were transfected with the cDNA. The cDNA-specific transport was calculated by adjusting for the endogenous activity. The kinetic parameters, Michaelis-Menten constant (K_t) and maximal velocity (V_{max}), were calculated by fitting the cDNA-specific transport data to the Michaelis-Menten equation describing a single saturable transport system. The Na^+- and Cl^--activation kinetics were analyzed by fitting the cDNA-specific transport data to the Hill equation, and the Hill coefficient was calculated.

Functional expression $ATB^{0,+}$ in Xenopus laevis oocytes. Capped cRNA from the cloned mouse $ATB^{0,+}$ cDNA was synthesized using the mMESSAGE mMACHINE kit (Ambion Inc., Austin, Texas, USA). Mature oocytes from *Xenopus laevis* were isolated by treatment with collagenase A (1.6 mg/ml), manually defolliculated, and maintained at 18°C in modified Barth's medium supplemented with 10 mg/ml gentamycin (23–25). On the following day, oocytes were injected with 50 ng cRNA. Uninjected oocytes served as controls. The oocytes were used for electrophysiological studies 6 days after cRNA injection. Electrophysiological studies were performed by the two-microelectrode voltage-clamp method (23–25). Oocytes were perifused with a NaCl-containing buffer (100 mM NaCl, 2 mM KCl, 1 mM $MgCl_2$, 1 mM $CaCl_2$, 3 mM HEPES, 3 mM Mes, and 3 mM Tris, pH 7.5), followed by the same buffer containing different NOS inhibitors or amino acids. The membrane potential was clamped at –50 mV. Voltage pulses between +50 and –150 mV, in 20-mV increments, were applied for 100-ms durations, and steady-state currents were measured. The differences between the steady-state currents measured in the presence and absence of substrates were considered as the substrate-induced currents. The kinetic parameter $K_{0.5}$ (i.e., the substrate

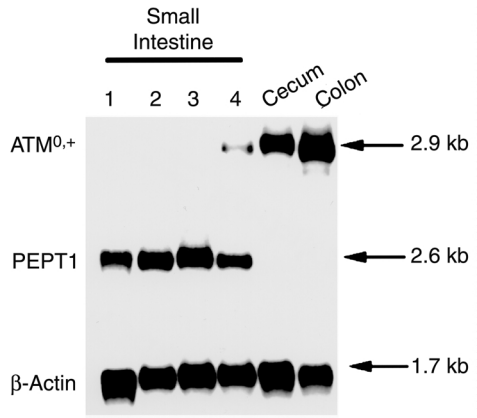

Figure 1
Northern blot analysis of ATB$^{0,+}$ mRNA along the longitudinal axis of the mouse intestinal tract. The small intestine was divided into four equal segments, the first segment representing the most proximal region and the fourth segment representing the most distal region of the small intestine. The blot was hybridized sequentially under high-stringency conditions with [^{32}P]-labeled cDNA probes specific for mouse ATB$^{0,+}$, mouse PEPT1, and mouse β-actin.

concentration necessary for the induction of half-maximal current) for the saturable transport of substrates was calculated by fitting the values of the substrate-induced currents to the Michaelis-Menten equation. The experiments were repeated with at least three different oocytes from two different batches.

Results

Structural features of mouse ATB$^{0,+}$. The cloned mouse ATB$^{0,+}$ cDNA obtained from colon mRNA is 3,007 bp-long (GenBank accession no. AF320226) and codes for a protein of 638 amino acids. The primary structure of mouse ATB$^{0,+}$ is highly homologous to the recently cloned human ATB$^{0,+}$ (26). The identity of amino acid sequence between the two proteins is 88%.

Expression pattern of ATB$^{0,+}$ mRNA in the mouse intestinal tract. To determine the expression pattern of ATB$^{0,+}$ along the longitudinal axis of the intestinal tract, we analyzed the steady-state levels of ATB$^{0,+}$ mRNA in different regions of the mouse intestine by Northern blot hybridization (Figure 1). ATB$^{0,+}$ mRNA was not detectable in the first three segments of the small intestine. The expression of the mRNA was, however, evident in the fourth segment of the small intestine, cecum, and colon. The mRNA levels were more abundant in the colon and cecum than in the distal small intestine. In contrast, mRNA for PEPT1, a H$^+$-coupled transporter for small peptides, was detectable in all four segments of the small intestine, but not in the cecum and colon. These data show that the expression of ATB$^{0,+}$ mRNA is restricted to the distal region of the mouse intestinal tract.

Functional features of mouse ATB$^{0,+}$. The functional identity of the cloned mouse ATB$^{0,+}$ cDNA was established first by expressing the clone in mammalian cells heterologously and studying its transport function. We studied the transport of several zwitterionic and cationic amino acids in human retinal pigment epithelial (HRPE) cells expressing the cloned mouse ATB$^{0,+}$. The transport of these amino acids was also measured under identical conditions in cells transfected with vector alone to serve as a control for endogenous transport activity. The transport activity of all 13 amino acids tested (Gly, Ala, Ser, Thr, Pro, His, Gln, Asn, Leu, Ile, Phe, Trp, and Arg) was found to be significantly higher in mouse ATB$^{0,+}$ cDNA-transfected cells than in vector-transfected cells (data not shown). The cDNA-induced increase in transport activity varied between 16 to 190% for all amino acids, except for glycine. The transport of glycine was exceptionally high in cDNA-transfected cells. The increase was 38-fold compared with transport activity in vector-transfected cells.

Since the transport of glycine via mouse ATB$^{0,+}$ was markedly higher compared with the transport of other amino acids, we used glycine as the substrate for further characterization of the cloned transporter. The results given in Figure 2 represent only the ATB$^{0,+}$-specific transport activity after correcting for the endogenous transport activity. The ATB$^{0,+}$-mediated glycine transport was obligatorily dependent on the presence of Na^+ and Cl^-. The transport of glycine via mouse ATB$^{0,+}$ was saturable with a Michaelis-Menten constant (K_t) of 210 ± 18 μM. The number of Na^+ and Cl^- ions

Table 1
Amino acid substrate specificity of mouse ATB$^{0,+}$

Unlabeled amino acid	mATB$^{0,+}$-specific [^{3}H]-glycine transport (pmol/10^6 cells/15 min)	(%)
Control	37.27 ± 1.20	100
Glycine	1.88 ± 0.06	5
Alanine	1.04 ± 0.05	3
Cysteine	1.11 ± 0.20	3
Serine	1.99 ± 0.09	5
Threonine	3.91 ± 0.30	11
Proline	9.97 ± 0.57	27
Histidine	1.31 ± 0.10	4
Glutamine	2.39 ± 0.18	6
Asparagine	3.25 ± 0.23	9
Leucine	0.27 ± 0.03	1
Isoleucine	0.27 ± 0.02	1
Phenylalanine	0.56 ± 0.03	2
Tryptophan	0.37 ± 0.06	1
Arginine	7.14 ± 0.35	19
Lysine	3.52 ± 0.28	9
Aspartate	32.01 ± 1.29	86
Glutamate	33.47 ± 0.91	90
MeAIB	36.21 ± 4.80	97

Transport of [^{3}H]-glycine (60 nM) was measured in vector-transfected HRPE cells and in mATB$^{0,+}$ cDNA-transfected HRPE cells at 37°C for 15 minutes in the presence of NaCl (pH 7.5). Unlabeled amino acids were used at a concentration of 2.5 mM. The cDNA-specific transport was calculated by subtracting the transport in vector-transfected cells from the transport in mATB$^{0,+}$ cDNA-transfected cells. Data (means ± SEM from four separate determinations) represent only cDNA-specific transport.

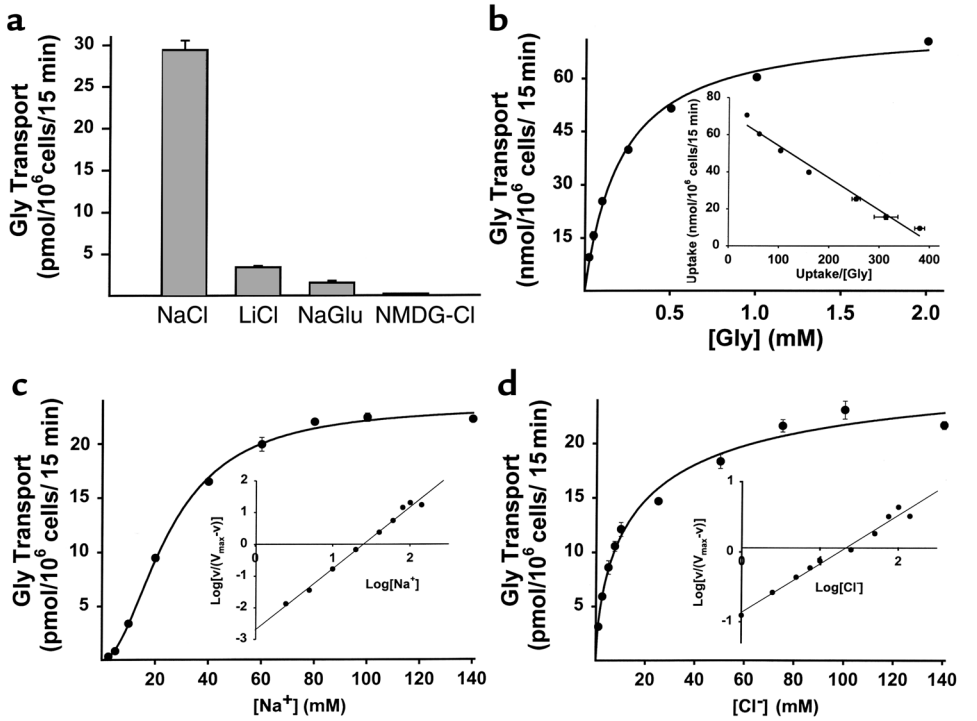

Figure 2
Functional characteristics of mouse $ATB^{0,+}$ in a mammalian cell–expression system with glycine as the substrate. Results represent only $ATB^{0,+}$-specific transport activity, which was calculated by subtracting the transport in vector-transfected cells from the transport in cDNA-transfected cells. (**a**) Ion-dependence of $ATB^{0,+}$-mediated glycine (60 nM) transport. (**b**) Saturation kinetics of $ATB^{0,+}$-mediated glycine transport. (**c**) Na^+-activation kinetics of $ATB^{0,+}$-mediated glycine (60 nM) transport. (**d**) Cl^--activation kinetics of $ATB^{0,+}$-mediated glycine (60 nM) transport.

involved in the transport process was then analyzed by the Na^+-activation kinetics and the Cl^--activation kinetics. The transport activity of mouse $ATB^{0,+}$ was sigmoidally related to the concentration of Na^+, and the Hill coefficient for the activation process for Na^+ was 2.0 ± 0.1. In contrast, the transport activity of mouse $ATB^{0,+}$ showed a hyperbolic relationship with the concentration of Cl^-. The Hill coefficient for the activation process for Cl^- was 0.7 ± 0.1. These results show that the Na^+/Cl^-/glycine stoichiometry is 2:1:1. The $K_{0.5}$ values for Na^+ and Cl^- (i.e., the concentrations of these ions needed for inducing half-maximal transport activity) were 25 ± 1 and 18 ± 8 mM, respectively.

The amino acid specificity of mouse $ATB^{0,+}$ was then studied by assessing the ability of a variety of amino acids to compete with [^{3}H]-glycine (60 nM) for the transport process mediated by the cloned transporter (Table 1). At a concentration of 2.5 mM, all zwitterionic and cationic amino acids tested inhibited the transport of [^{3}H]-glycine mediated by mouse $ATB^{0,+}$. The inhibition varied from 70 to 100%. In contrast, the anionic amino acid aspartate and the *N*-methylated amino acid, α-(methylamino)isobutyric acid (MeAIB), did not show any significant inhibition. These data show that the cloned mouse $ATB^{0,+}$ is capable of mediating the transport of zwitterionic and cationic amino acids in a Na^+- and Cl^--coupled manner.

Transport of NOS inhibitors via $ATB^{0,+}$. We then assessed the ability of NOS inhibitors and their parent amino acids (arginine, lysine, ornithine, and citrulline) at a concentration of 2.5 mM to compete with [^{3}H]-glycine (10 μM) for the transport process mediated by mouse $ATB^{0,+}$ in HRPE cells (Table 2). All four parent amino acids caused marked inhibition of glycine transport via mouse $ATB^{0,+}$. The inhibition varied between 55 and 85%. Similarly, all NOS inhibitors that were tested also inhibited $ATB^{0,+}$-mediated glycine transport. The inhibition caused by the arginine-based NOS inhibitors L-NNA; N^G-nitro-L-arginine methyl ester (L-NAME); N^G-monomethyl-L-homoarginine (L-NMMHA); N^G,N^G-dimethyl-L-arginine (L-NDMA); N^G-monoethyl-L-arginine (L-NMEA); N^G-monomethyl-L-arginine (L-NMMA); and N^G-L-nitro-L-arginine benzyl ester (L-NABE) was in the range of 30–80%. The lysine-based NOS inhibitor L-N^6-(1-iminoethyl)-lysine (L-NIL) caused 35% inhibition. L-Thiocitrulline (L-TC) and S-methyl-L-thiocitrulline (L-MTC), the citrulline-based NOS inhibitors, were very potent as inhibitors of $ATB^{0,+}$-mediated glycine transport, the inhibition being in the range of 70–85%. The ornithine derivative L-N^5-(1-iminoethyl)-ornithine (L-NIO) caused 40% inhibition. L-Canavanine and α-guanidinoglutaric acid (L-GGA), both being guanidino derivatives, were also effective inhibitors, causing 75 and 40% inhibition, respectively.

Figure 3 describes the dose-response relationship for the inhibition of $ATB^{0,+}$-mediated glycine transport by six of the NOS inhibitors. The inhibitory potency was in the following order: L-TC > L-NNA > L-MTC = L-

NMMA > L-NIO = L-NIL. The IC_{50} values (i.e., the concentration of the compound necessary to cause 50% inhibition) were as follows: L-TC (0.21 ± 0.03 mM), L-NNA (0.56 ± 0.04 mM), L-MTC (0.73 ± 0.09 mM), L-NMMA (0.77 ± 0.12 mM), L-NIO (2.65 ± 0.25 mM), and L-NIL (2.60 ± 0.29 mM).

These results show that all NOS inhibitors tested interact with the substrate-binding site of the cloned mouse $ATB^{0,+}$. However, these data suggest but do not prove that these NOS inhibitors are transportable substrates for the transporter. It is possible that some compounds may block the transport by competing with glycine for binding to the substrate-binding site without itself being transported across the membrane. To determine whether or not these inhibitors are actually transportable substrates of the transporter, direct measurements of $ATB^{0,+}$-mediated transport of these inhibitors must be carried out. Toward this goal we used [^{3}H]-L-NNA as a substrate for $ATB^{0,+}$ and studied its transport in HRPE cells expressing the cloned transporter (Figure 4). The transport of L-NNA in $ATB^{0,+}$-expressing cells was fourfold higher than in vector-transfected cells, demonstrating that L-NNA is indeed a transportable substrate for this transporter. This conclusion is supported further by the inhibition of $ATB^{0,+}$-specific L-NNA transport by glycine, serine, and arginine that are substrates for the transporter. In contrast, MeAIB and glutamate that are not substrates for the transporter did not inhibit $ATB^{0,+}$-specific L-NNA transport. The $ATB^{0,+}$-specific L-NNA transport was saturable with a Michaelis-Menten constant of 0.75 ± 0.10 mM.

The mammalian expression system is not ideal to use in the investigation of the transport of a broad spectrum of NOS inhibitors via $ATB^{0,+}$ because of the limited commercial availability of NOS inhibitors in radiolabeled form. Therefore, we had to use an alternative method for direct measurement of the transport of a large number of NOS inhibitors via $ATB^{0,+}$. We used the *X. laevis* oocyte expression system for this purpose. The cloned mouse $ATB^{0,+}$ was functionally expressed in these oocytes by injection of cRNA, and the transport of NOS inhibitors (1 mM) via the transporter was then monitored by inward currents induced by these inhibitors using the two-microelectrode voltage-clamp technique. This approach was feasible because of the electrogenic nature of $ATB^{0,+}$. Induction of an inward current upon exposure of the $ATB^{0,+}$-expressing oocyte to a test compound under voltage-clamped conditions would indicate depolarization of the membrane as a result of transport of the compound into the oocyte. Uninjected oocytes served as negative controls in these experiments. The results of these oocyte experiments are given in Table 2. All of the NOS inhibitors tested, except for L-NAME, L-NABE, and L-GGA, induced marked inward currents in oocytes expressing the cloned $ATB^{0,+}$. The currents varied in the range of 30–500 nA. Comparatively, L-NAME, L-NABE, and L-GGA induced very little current (10–15 nA). The amino acids arginine, lysine, citrulline, and ornithine induced currents in the range of 130–550 nA.

For further detailed analysis of the transport of NOS inhibitors via $ATB^{0,+}$ in the oocyte expression system,

Table 2
Transport of NOS inhibitors via mouse $ATB^{0,+}$

Unlabeled amino acid or NOS inhibitor	$mATB^{0,+}$-specific [^{3}H]-glycine transport in HRPE cells	Current in *X. laevis* oocytes
	nmol/10^6 cells/15 min	nA
Control	7.29 ± 0.08 (100)	
Arginine	2.21 ± 0.05 (30)	382 ± 57
Lysine	1.48 ± 0.02 (20)	545 ± 95
Citrulline	1.10 ± 0.01 (15)	498 ± 114
Ornithine	3.28 ± 0.01 (45)	131 ± 27
L-NNA	1.54 ± 0.03 (21)	200 ± 92
L-NAME	5.25 ± 0.10 (72)	11 ± 2
L-NMMHA	5.21 ± 0.06 (72)	33 ± 6
L-NDMA	4.25 ± 0.10 (58)	85 ± 15
L-NMEA	3.77 ± 0.17 (52)	138 ± 16
L-NMMA	2.60 ± 0.06 (36)	411 ± 76
L-NABE	4.93 ± 0.19 (67)	16 ± 2
L-NIL	4.77 ± 0.73 (65)	89 ± 18
L-TC	1.05 ± 0.06 (15)	497 ± 104
L-MTC	2.03 ± 0.09 (28)	118 ± 34
L-NIO	4.17 ± 0.10 (57)	71 ± 16
L-Canavanine	1.75 ± 0.03 (24)	269 ± 73
GGA	4.22 ± 0.09 (58)	7 ± 1

Transport of [^{3}H]-glycine (10 μM) was measured in vector-transfected HRPE cells and in $mATB^{0,+}$ cDNA-transfected HRPE cells at 37°C for 15 minutes in the presence of NaCl (pH 7.5). Unlabeled amino acids and NOS inhibitors were used at a concentration of 2.5 mM. cDNA-specific transport was calculated by subtracting the transport in vector-transfected cells from the transport in $mATB^{0,+}$ cDNA-transfected cells. Values in parenthesis are percent of control transport. Data (means ± SEM from four separate determinations) represent only cDNA-specific transport. Mouse $ATB^{0,+}$ was also expressed in *X. laevis* oocytes by injecting $mATB^{0,+}$ cRNA, and the inward currents induced by amino acids and NOS inhibitors (1 mM) were measured using the two-microelectrode voltage-clamp technique. The perifusion medium contained NaCl (pH 7.5). Data represent means ± SEM from three different batches of oocytes.

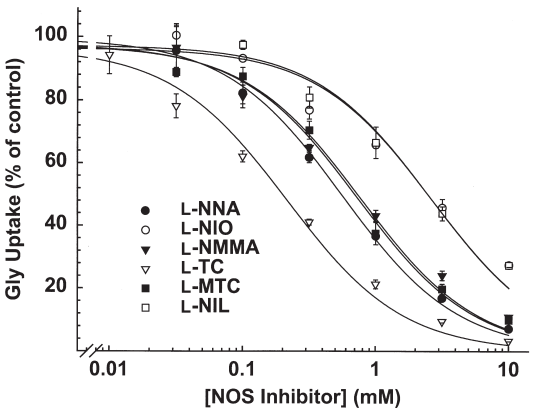

Figure 3
Dose-response relationship for the inhibition of $ATB^{0,+}$-specific glycine (10 μM) transport by NOS inhibitors in HRPE cells expressing the cloned mouse $ATB^{0,+}$.

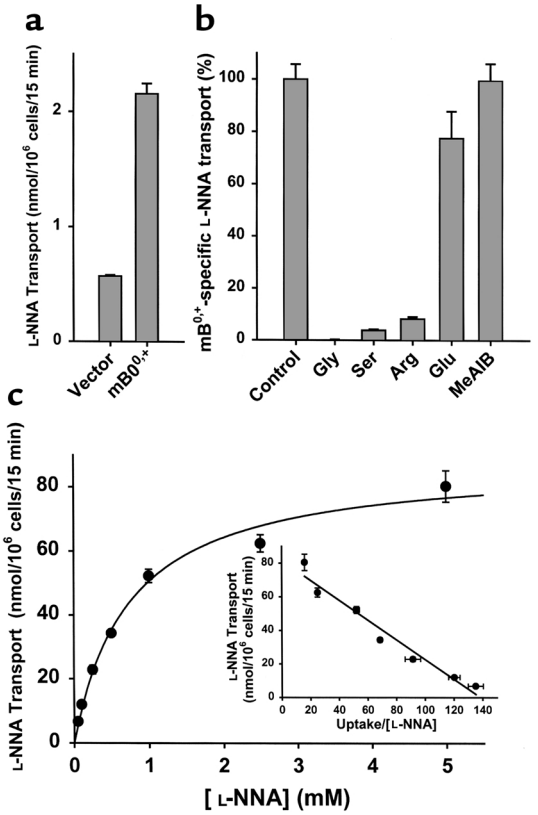

Figure 4
Characteristics of L-NNA transport via $ATB^{0,+}$. The cloned mouse $ATB^{0,+}$ was expressed in HRPE cells, and the transport of [^{3}H]-L-NNA (10 μM) was studied. Results represent only $ATB^{0,+}$-specific transport. (**a**) Transport of L-NNA in vector-transfected cells and in $ATB^{0,+}$ cDNA-transfected cells. (**b**) Inhibition of $ATB^{0,+}$-specific L-NNA transport by amino acids (5 mM). (**c**) Saturation kinetics of L-NNA transport via $ATB^{0,+}$.

we selected three NOS inhibitors, namely L-NIL, L-MTC, and L-NIO. We chose these compounds on the basis of their selectivity toward distinct NOS isoforms: L-NIL for NOS II, L-MTC for NOS I, and L-NIO for NOS III. Figure 5 describes the ion dependence of the inward currents induced by L-NIL and L-MTC. In the presence of NaCl, L-NIL at a concentration of 1 mM induced 82 ± 18 nA inward currents. However, when measured in the presence of NMDG chloride, there was no measurable inward current upon exposure of the oocytes to this compound, indicating that the L-NIL–induced currents were obligatorily dependent on the presence of Na^+. This compound did induce a small, but significant, current (~10 nA) in the presence of sodium gluconate (i.e., in the absence of chloride). However, since L-NIL used in this experiment was a chloride salt, a small amount of chloride was present under these experimental conditions. This resulted in the induction of the observed current. This is supported by the data obtained with L-MTC, which is available in a chloride-free form. In the presence of NaCl, L-MTC at a concentration of 1 mM induced 116 ± 34 nA inward currents. But there were no measurable currents when either Na^+ or Cl^- was absent, showing that the L-MTC–induced inward current was absolutely dependent on the presence of both Na^+ and Cl^-. The obligatory dependence of the currents induced by L-NIL and L-MTC on the presence of Na^+ and Cl^- was similar to the data obtained with arginine. When used as a chloride-free salt, arginine induced 382 ± 57 nA inward current. No measurable current was observed with arginine in the absence of either Na^+ or Cl^-.

We then analyzed the saturation kinetics of the transport of L-MTC, L-NIL, and L-NIO via $ATB^{0,+}$ in the oocyte expression system using the inward currents induced by the corresponding inhibitors as the measure of their transport. The results of these experiments, shown in Figure 6, demonstrate that $ATB^{0,+}$-mediated transport of all three compounds was saturable. The $K_{0.5}$ values (the concentration of the compound necessary to induce half-maximal current) calculated at membrane potential –50 mV were 1.36 ± 0.08 mM, 2.72 ± 0.29 mM, and 2.24 ± 0.35 mM for L-MTC, L-NIL, and L-NIO, respectively. The $K_{0.5}$ values were, however, influenced by the membrane potential for all three compounds. The values decreased with hyperpolarization of the membrane and increased with depolarization of the membrane.

Discussion

In this article we present evidence for the transport of NOS inhibitors via the Na^+- and Cl^--coupled $ATB^{0,+}$. This represents the first identification of an ion gradient–

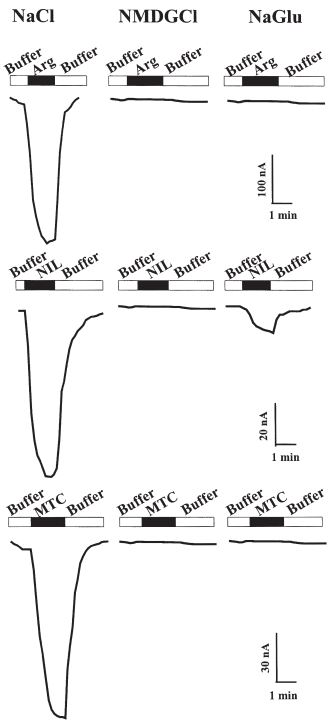

Figure 5
Ion dependence of inward currents induced by L-arginine, L-NIL, and L-MTC in *X. laevis* oocytes expressing the cloned mouse $ATB^{0,+}$. Oocytes were perifused with 1 mM substrates in buffers containing NaCl, sodium gluconate, or NMDG chloride.

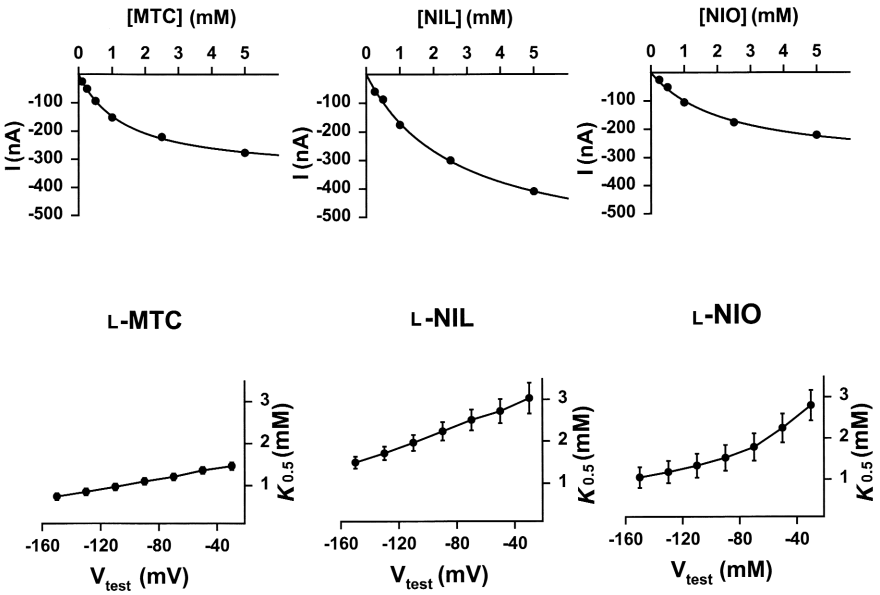

Figure 6
Saturation kinetics for NOS inhibitors for transport via $ATB^{0,+}$ in *X. laevis* oocyte expression system. Oocytes expressing the cloned mouse $ATB^{0,+}$ were perifused with increasing concentrations of L-MTC, L-NIL, and L-NIO, and the inward currents were measured under voltage-clamp conditions. Upper panels represent the relationship between substrate concentration and inward current at –50 mV. Lower panels represent the relationship between $K_{0.5}$ values and membrane potential.

driven concentrative transport system for these potential therapeutic agents. The evidence in support of $ATB^{0,+}$-mediated transport of NOS inhibitors was obtained with $ATB^{0,+}$ cloned from the mouse colon. The transport function of the cloned $ATB^{0,+}$ was studied by heterologous expression in mammalian cells as well as in *X. laevis* oocytes. This approach enabled us to investigate directly the transport of a wide variety of NOS inhibitors via the transporter. NOS inhibitors can be either cationic or zwitterionic in nature. Previous studies have shown that cationic NOS inhibitors are transported by system y^+ whereas zwitterionic NOS inhibitors are transported by system L (17–21). System y^+ does not interact with zwitterionic NOS inhibitors and system L does not interact with cationic NOS inhibitors. Our present studies show that $ATB^{0,+}$ is able to transport both cationic as well as zwitterionic NOS inhibitors. This is in accordance with the substrate specificity of this transporter. $ATB^{0,+}$ recognizes cationic amino acids as well as zwitterionic amino acids as substrates. Among the amino acid substrates of $ATB^{0,+}$, how the amino acids arginine, lysine, citrulline, and ornithine are handled by the transporter is directly relevant to the present study because most of the NOS inhibitors that are currently in investigational use are structurally related to these four amino acids. Even though arginine, lysine, and ornithine are cationic and citrulline is zwitterionic, our present studies show that all of these four amino acids are transportable substrates for $ATB^{0,+}$. Similarly, most NOS inhibitors, whether cationic or zwitterionic, that are structurally related to the four amino acids are transported via $ATB^{0,+}$.

Among the three amino acid transporters that are known thus far to recognize NOS inhibitors as substrates, $ATB^{0,+}$ is the most concentrative. This transporter is energized by the combined transmembrane gradients of Na^+ and Cl^-, as well as membrane potential. In contrast, system y^+ is driven only by membrane potential and system L is most likely facilitative, with no known driving force. Therefore, the transport of NOS inhibitors into cells that express $ATB^{0,+}$ is likely to be highly concentrative. The intracellular concentration of the NOS inhibitors in these cells can potentially reach several-fold higher than the extracellular concentration.

We determined the affinity of six NOS inhibitors for $ATB^{0,+}$ in the mammalian cell expression system from their ability to compete with an amino acid substrate for the transport process. These are L-NNA and L-NMMA (both structurally related to arginine), L-NIL (structurally related to lysine), L-TC and L-MTC (both structurally related to citrulline), and L-NIO (structurally related to ornithine). The IC_{50} values for these six compounds varied within the range of 0.2–2.7 mM. In the case of L-NNA, we also determined the affinity directly from its transport via $ATB^{0,+}$ in the same mammalian cell–expression system. The constant K_t calculated from the direct measurement of transport was found to be very similar to the IC_{50} value calculated from the competitive inhibition studies (0.75 ± 0.10 mM vs. 0.56 ± 0.04 mM). For three other NOS inhibitors (L-MTC, L-NIL, and L-NIO), we determined the Michaelis-Menten constant for their transport via $ATB^{0,+}$ using the *X. laevis* oocyte-expression system. The K_t values calculated from these experiments were found to be similar to the corresponding IC_{50} values determined from the competitive inhibition studies using the mammalian cell–expression system (1.36 ± 0.08

mM vs. 0.73 ± 0.09 mM for L-MTC; 2.72 ± 0.29 mM vs. 2.60 ± 0.29 mM for L-NIL; and 2.24 ± 0.35 mM vs. 2.65 ± 0.25 mM for L-NIO).

The transport of NOS inhibitors via $ATB^{0,+}$ is of significant pharmacological and clinical relevance. This suggests that $ATB^{0,+}$ has the potential for use as a drug-delivery system for NOS inhibitors. We cloned $ATB^{0,+}$ from the mouse colon. But, there is ample evidence for the expression of this transport system not only in the colon but also in the distal small intestine (16, 27). The transport function has been shown to be present in the brush border membrane of the mucosal cells in the ileum (16, 27). $ATB^{0,+}$ mRNA is detectable in the present study only in the distal regions of the intestinal tract (ileum, cecum, and colon). The expression pattern of $ATB^{0,+}$ mRNA along the longitudinal axis of the intestinal tract is interesting and of relevance to the potential use of this transporter as a delivery system for NOS inhibitors. To our knowledge, the restricted expression of $ATB^{0,+}$ in the distal intestinal tract is unique among the amino acid transporters. Amino acids derived from the dietary proteins are absorbed mostly in the proximal small intestine, and consequently the concentrations of amino acids in the distal regions of the intestinal tract are low. As a result, there will be little competition between NOS inhibitors and endogenous amino acids for transport via $ATB^{0,+}$. This will enhance the efficiency of intestinal absorption of NOS inhibitors.

There are two other amino acid transport systems in the intestinal brush border membrane that may participate in the uptake of NOS inhibitors from the intestinal lumen. These are system y^+ and system $b^{0,+}$. The ability of system y^+ to transport cationic NOS inhibitors has been well established. In contrast, there is very little information available on the ability of system $b^{0,+}$ to transport NOS inhibitors. Since this transport system is able to interact with zwitterionic as well as cationic amino acids, we predict that this system can handle zwitterionic as well as cationic NOS inhibitors. Our recent studies have indeed demonstrated that system $b^{0,+}$ is at least partly responsible for the uptake of the zwitterionic NOS inhibitor L-NNA across the intestinal brush border membrane (22). However, both system y^+ and system $b^{0,+}$ are not driven by any ion gradient. Therefore, we speculate that $ATB^{0,+}$, with its energetic coupling to transmembrane gradients of Na^+ and Cl^-, is likely to be much more efficient than system y^+ and system $b^{0,+}$ in the uptake of NOS inhibitors from the lumen into the intestinal and colonic absorptive cells.

The oral bioavailability of NOS inhibitors will depend not only on the existence of entry routes for these compounds in the intestinal and colonic brush border membrane, but also on the existence of exit routes in the basolateral membrane. There are two amino acid transport systems in the basolateral membrane of the intestinal tract that may be of relevance to the exit of NOS inhibitors from the intestinal and colonic absorptive cells into the blood. These are system L and system y^+L (16). The NOS inhibitors that are absorbed into the intestinal and colonic epithelial cells via $ATB^{0,+}$, system y^+, and system $b^{0,+}$, can exit these cells across the basolateral membrane via systems L and y^+L.

The present studies may also be of clinical relevance to the management of intestinal and colonic inflammation with NOS inhibitors. There is convincing evidence for the induction of NOS II in the intestinal and colonic epithelial cells during inflammation (28, 29). Nitric oxide plays an important role in the normal physiological function of the intestinal tract and also in pathological conditions such as bacterial sepsis and inflammatory bowel disease (30). It is of interest to note that the inflammatory bowel diseases ulcerative colitis and Crohn's disease involve primarily the colon and/or ileum, the sites at which $ATB^{0,+}$ is principally expressed in the intestinal tract. The idea of using $ATB^{0,+}$ as the delivery system for NOS inhibitors is particularly appealing for several reasons with respect to the clinical management of inflammatory bowel disease in which there is an induction of NOS II in the intestinal and colonic epithelial cells. $ATB^{0,+}$ is a highly concentrative transporter, and therefore the NOS inhibitors will be absorbed very effectively into the intestinal and colonic epithelial cells and accumulated inside the cells at high concentrations. This will result in an effective means of inhibiting NOS II in these cells. Furthermore, NOS inhibitors in the intestinal lumen will compete with arginine, the substrate for NOS II, for transport into the cells via $ATB^{0,+}$ and thus reduce the availability of arginine for NOS II activity. Thus, $ATB^{0,+}$ will allow NOS inhibitors to get into the cells in place of arginine. This will result in a very effective inhibition of NOS II activity, both by reducing the availability of arginine, the NOS II substrate, and by increasing the intracellular concentration of NOS inhibitors.

Acknowledgments

This work was supported by NIH grant GM-54122.

1. Moncada, S. 1999. Nitric oxide: discovery and impact on clinical medicine. *J. R. Soc. Med.* **92**:164–169.
2. Martin, E., Davis, K., Bian, K., Lee, Y.C., and Murad, F. 2000. Cellular signaling with nitric oxide and cyclic guanosine monophosphate. *Semin. Perinatol.* **24**:2–6.
3. Bredt, D.S. 1999. Endogenous nitric oxide synthesis: biological functions and pathophysiology. *Free Radic. Res.* **31**:577–596.
4. Knowles, R.G., and Moncada, S. 1994. Nitric oxide synthases in mammals. *Biochem. J.* **298**:249–258.
5. Stuehr, D.J. 1999. Mammalian nitric oxide synthases. *Biochim. Biophys. Acta.* **1411**:217–230.
6. Miller, M.J.S., and Grisham, M.B. 1995. Nitric oxide as a mediator of inflammation? You had better believe it. *Mediators Inflamm.* **4**:387–396.
7. Symeonides, S., and Balk, R.A. 1999. Nitric oxide in the pathogenesis of sepsis. *Infect. Dis. Clin. North Am.* **13**:449–463.
8. Mandrup-Poulsen, T. 1996. The role of interleukin-1 in the pathogenesis of IDDM. *Diabetologia.* **39**:1005–1029.
9. Jenner, P., and Olanow, C.W. 1996. Oxidative stress and the pathogenesis of Parkinson's disease. *Neurology.* **47**:S161–S170.
10. Southan, G.J., and Szabo, C. 1996. Selective pharmacological inhibition of distinct nitric oxide synthase isoforms. *Biochem. Pharmacol.* **51**:383–394.

11. Bryk, R., and Wolff, D.J. 1999. Pharmacological modulation of nitric oxide synthesis by mechanism-based inactivators and related inhibitors. *Pharmacol. Ther.* **84**:157–178.
12. Moncada, S., and Higgs, E.A. 1995. Molecular mechanisms and therapeutic strategies related to nitric oxide. *FASEB J.* **9**:1319–1330.
13. Hobbs, A.J., Higgs, A., and Moncada, S. 1999. Inhibition of nitric oxide synthase as a potential therapeutic target. *Annu. Rev. Pharmacol. Toxicol.* **39**:191–220.
14. Christensen, H.N. 1989. Distinguishing amino acid transport systems of a given cell or tissue. *Methods Enzymol.* **173**:576–616.
15. Palacin, M., Estevez, R., Bertran, J., and Zorzano, A. 1998. Molecular biology of mammalian plasma membrane amino acid transporters. *Physiol. Rev.* **78**:969–1054.
16. Ganapathy, V., Ganapathy, M.E., and Leibach, F.H. 2001. Intestinal transport of peptides and amino acids. In *Current topics in membranes*. Volume 50. K.E. Barrett and M. Donowitz, editors. Academic Press. San Diego, California, USA. 379–412.
17. Schmidt, K., Klatt, P., and Mayer, B. 1993. Characterization of endothelial cell amino acid transport systems involved in the actions of nitric oxide synthase inhibitors. *Mol. Pharmacol.* **44**:615–621.
18. Schmidt, K., Klatt, P., and Mayer, B. 1994. Uptake of nitric oxide synthase inhibitors by macrophage RAW 264.7 cells. *Biochem. J.* **301**:313–316.
19. Baydoun, A.R., and Mann, G.E. 1994. Selective targeting of nitric oxide synthase inhibitors to system y^+ in activated macrophages. *Biochem. Biophys. Res. Commun.* **200**:726–731.
20. Schmidt, K., List, B.M., Klatt, P., and Mayer, B. 1995. Characterization of neuronal amino acid transporters: uptake of nitric oxide synthase inhibitors and implication for their biological effects. *J. Neurochem.* **64**:1469–1475.
21. Raghavendra Rao, V.L., and Butterworth, R.F. 1996. L-[^{3}H]-nitroarginine and L-[^{3}H]-arginine uptake into rat cerebellar synaptosomes: kinetics and pharmacology. *J. Neurochem.* **67**:1275–1281.
22. Hatanaka, T., Nabuchi, Y., and Ushio, H. 1999. Transport of N^G-nitro-L-arginine across intestinal brush border membranes by Na^+-dependent and Na^+-independent amino acid transporters. *Pharm. Res.* **16**:1770–1774.
23. Sugawara, M., et al. 2000. Cloning of an amino acid transporter with functional characteristics and tissue expression pattern identical to that of system A. *J. Biol. Chem.* **275**:16473–16477.
24. Fei, Y.J., et al. 2000. Primary structure, genomic organization, and functional and electrogenic characteristics of human system N (SN1), a Na^+- and H^+-coupled glutamine transporter. *J. Biol. Chem.* **275**:23707–23717.
25. Wang, H., et al. 2000. Structure, function, and genomic organization of human Na^+-dependent high-affinity dicarboxylate transporter. *Am. J. Physiol. Cell Physiol.* **278**:C1019–C1030.
26. Sloan, J.L., and Mager, S. 1999. Cloning and functional expression of a human Na^+ and Cl^--dependent neutral and cationic amino acid transporter $B^{0,+}$. *J. Biol. Chem.* **274**:23740–23745.
27. Munck, L.K. 1995. Chloride-dependent amino acid transport in the small intestine: occurrence and significance. *Biochim. Biophys. Acta.* **1241**:195–213.
28. Tepperman, B.L., Brown, J.F., and Whittle, B.J.R. 1993. Nitric oxide synthase induction and intestinal epithelial cell viability in rats. *Am. J. Physiol. Gastrointest. Liver Physiol.* **265**:G214–G218.
29. Singer, I.I., et al. 1996. Expression of nitric oxide synthase and nitrotyrosine in colonic epithelium in inflammatory bowel disease. *Gastroenterology.* **111**:871–875.
30. Stensen, W.F. 1999. Gastrointestinal inflammation. In *Textbook of gastroenterology.* T. Yamada, editor. Lippincott Williams & Wilkins. Philadelphia, Pennsylvania, USA. 123–140.